Chaos, Solitons & Fractals 68 (2014) 65–71

Contents lists available at ScienceDirect

Chaos, Solitons & Fractals

Nonlinear Science, and Nonequilibrium and Complex Phenomena

journal homepage: www.elsevier.com/locate/chaos

Quantification of synchronization phenomena in two reciprocally gap-junction coupled bursting pancreatic β-cells

Jing Wang, Shenquan Liu *, Xuanliang Liu

School of Mathematics, South China University of Technology, Guangzhou 510640, China

ARTICLE INFO

Article history:
Received 21 March 2014
Accepted 25 July 2014
Available online 24 August 2014

ABSTRACT

This paper aims to discuss our research into synchronized transitions in two reciprocally gap-junction coupled bursting pancreatic β-cells. Numerical results revealed that propagations of synchronous states could be induced not only by changing the coupling strength, but also by varying the slow time constant. Firstly, these asynchronous and synchronous states such as out-of-phase, almost in-phase and in-phase synchronization were specifically demonstrated by phase portraits and time evolutions. By comparing interspike intervals (ISI) bifurcation diagrams of two coupled neurons with an individual neuron, we found that coupling strength played a critical role in tonic-to-bursting transitions. In particular, with the phase difference and ISI-distance being introduced, regions of various synchronous and asynchronous states were plotted in a two-dimensional parameter space. More interestingly, it was found that the coupled neurons could always realize complete synchronization as long as the coupling strength was appropriate.

1. Introduction

As we all know, neuronal synchronization plays a significant role in pathophysiological processes occurring in Parkinson's disease [1] and during epileptic seizures [2]. The transitions of synchronization states are of vital importance in neuronal networks. In the past decades, many investigations into neural synchronization have been conducted [3–8], and some important methods were proposed to bring fundamental new insights into the principles of synchronization [9–13]. Arenas et al. [3] reported advances in the understanding of synchronization phenomena in a complex network topology. Volman et al. [4] researched the role of electrical synapses in the synchronization of neuronal ensembles and the link between gap junctions and epilepsy. The dependence of synchronization transitions over scale-free neuronal networks with attractive and repulsive coupling was investigated in Ref. [5]. The variable higher-order coupling term, bursting oscillations and corresponding bifurcation in the modified Morris–Lecar neuron and the effect of time delay in the coupled FHN models were studied in Refs. [6–8]. Postnova et al. [9] used the analysis of phase difference to investigate the classification of synchronous states. Pikovsky et al. [10] illustrated synchronization phenomena in combined oscillators and in spatially distributed systems from both qualitative and quantitative perspectives. Ermentrout [11] adopted singular perturbation theory and the phase resetting curve to research the property of Type 1 membrane models. Chow et al. [12] showed that spike shape and size were of importance in the existence and stability of phase-locked modes of electrically coupled neurons. Hansel et al. [13] studied synchronization properties of all-to-all coupled identical neurons with purely excitatory interactions and showed that there were two distinct types of responses dependent on the time course of synaptic interactions and the response of coupled neurons to small depolarizations.

* Corresponding author. Tel.: +86 136 5082 3684.
E-mail address: mashqliu@scut.edu.cn (S. Liu).

http://dx.doi.org/10.1016/j.chaos.2014.07.012
0960-0779/

In neuronal systems, the coupling between neurons can be divided into two types: electrical coupling via gap junctions and chemical coupling via chemical synapses. For electrical coupling, the role of electrical synapses is reflected in synchronizing neuronal activity by adjusting its strength and physiological response [14,15]. While for chemical coupling, the synchronization process is mediated through regulating fast and slow synaptic transmission by the exchange of neurotransmitters [16,17]. Recently, research of the synchronization transitions in small-world and scale-free neuronal networks with hybrid electrical–chemical synapses have been performed by Wang et al. [18,19]. Additionally, the hybrid synapses have an advantage in signal detection and transmission in neuronal systems [20]. Sun et al. found that electrical coupling is more adept at transmitting signals, while chemical coupling is more suited to detecting signals.

The purpose of this present work is to analyze (1) how the coupling strength influences the discharge pattern of the neurons and (2) how the synchronous states transit from one to another. Here, we have chosen the model of pancreatic β-cell which has been simplified to three dimensions. In the previous studies of this model, Mosekilde et al. [21] studied the period-doubling and period-adding structure through the analysis of one- and two-dimensional bifurcation. Moreover, synchronization has been studied both in gap junction coupled cells [22,23] and in a ring neuronal network [24]. In this paper, we focus on extending the analysis of two coupled bursting pancreatic β-cells. First, we investigate several synchronous states while varying the coupling strength. Then, we compare the bifurcation diagrams of the coupled neurons with an isolated one. Finally, with the method of phase difference and ISI-distance, the analysis of synchronization becomes more comprehensive.

The paper is constituted as follows. In Section 2, we describe a simplified model of two electrically coupled pancreatic β-cells. The corresponding numerical simulation methods are introduced in Section 3. Section 4 shows the synchronization propagations of two coupled neurons with the variations of the coupling strength and the slow time constant. Finally, conclusions are given in Section 5.

2. Model description

Based on the minimal model proposed by Sherman et al. [25], we coupled two pancreatic β-cells via a gap junction. Each neuron contains three channels, namely calcium channels, potassium channels, and slow variable channels. The schematic diagram of the coupled neurons is shown in Fig. 1.

The synthetic dynamics of two coupled pancreatic β-cells are depicted by the following differential equations:

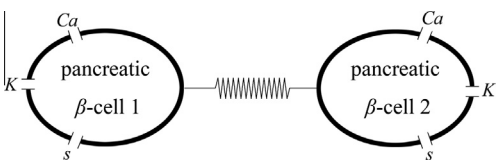

Fig. 1. Schematic diagram of two coupled pancreatic β-cells.

$$\tau dV_{1,2}/dt = -I_{Ca}(V_{1,2}) - I_K(V_{1,2}, n_{1,2}) - I_s(V_{1,2}, s_{1,2}) - g_c(V_{1,2} - V_{2,1}) \quad (1)$$

$$\tau dn_{1,2}/dt = \lambda(n_\infty(V_{1,2}) - n_{1,2}) \quad (2)$$

$$\tau_s ds_{1,2}/dt = s_\infty(V_{1,2}) - s_{1,2} \quad (3)$$

where variables V_i, n_i, and s_i $(i = 1, 2)$ represent the membrane potential, the opening probability of potassium channels, and a slow variable in this system, respectively, and the subscript 1 (or 2) indicates the first (or second) neuron. The parameter τ denotes the fast time constant for V and n; τ_s denotes the slow time constant for s. Each ionic current is defined by

$$I_{Ca}(V_{1,2}) = g_{Ca} m_\infty(V_{1,2})(V_{1,2} - V_{Ca}) \quad (4)$$

$$I_K(V_{1,2}, n_{1,2}) = g_K n_\infty(V_{1,2})(V_{1,2} - V_K) \quad (5)$$

$$I_s(V_{1,2}, s_{1,2}) = g_s s_\infty(V_{1,2})(V_{1,2} - V_K) \quad (6)$$

$$x_\infty(V_{1,2}) = 1/(1 + exp(-(V_{1,2} - V_x)/\theta_x)), x = m, n, s \quad (7)$$

where g_{Ca}, g_K and g_s represent the maximum conductance of I_{Ca}, I_K, and I_s, respectively; V_{Ca} and V_K stand for the reversal potentials of Ca^{2+} and K^+ ions, respectively; g_c is the coupling strength between two neurons.

The values of all parameters used in the above model are listed as follows: $\tau = 0.02$ s, $\tau_s = 16$ s, $g_{Ca} = 3.6$, $g_K = 10$, $g_s = 4$, $\lambda = 0.85$, $V_{Ca} = 25$ mV, $V_K = -75$ mV, $V_m = -20$ mV, $V_n = -16$ mV, $V_s = -38.34$ mV, $\theta_m = 12$ mV, $\theta_n = 5.6$ mV, $\theta_s = 10$ mV.

3. Methods

3.1. Phase difference

In order to better understand the synchronization transitions between two coupled pancreatic β-cells, the phase difference is introduced to distinguish different synchronous states, and it is calculated by:

$$\Delta\varphi = 2\pi(t_s - t_1)/(t_2 - t_1), t_1 < t_s \leqslant t_2 \quad (8)$$

where t_1 and t_2 denote the times of adjacent spikes of the first neuron and t_s is the spiking time of the second neuron [9].

3.2. ISI-distance

The ISI-distance proposed by Kreuz et al. [26–28] can be used to measure the synchronization degree of two coupled neurons, and it is measured using the following procedures. Firstly, we need to extract the spiking times by use of a spike detection algorithm. The spiking times are chosen when the membrane potential is greater than -35 mV threshold and is not less than the voltage of the surroundings. Secondly, the instantaneous interspike interval at each time is detected by:

$$x_{isi}(t) = min\{t_i^x | t_i^x > t\} - max\{t_i^x | t_i^x < t\}, \quad t_1^x < t < t_M^x \quad (9)$$

where t_i^x denotes the spiking times of the spike train $x_{isi}(t)$. Similarly we can get the second spike train t_i^y. Next, an appropriate normalization is adopted to compute the ratio between x_{isi} and y_{isi} as:

$$I(t) = (x_{isi}(t) - y_{isi}(t))/max(x_{isi}(t), y_{isi}(t)). \quad (10)$$

Finally, the time-weighted distance DI is integrated as:

$$DI = \int_{t=0}^{Time} dt|I(t)|. \quad (11)$$

The model is programed in Python using a fourth-order Runge–Kutta algorithm increasing in steps of 0.1 ms. All diagrams are drawn using matplotlib which is an open source library in Python.

4. Simulation results

4.1. The variation of coupling strength

Several synchronization states can be observed with the variation of the coupling strength. At $\tau_s = 16$ s, the following dynamical phenomena can be detected as shown in Fig. 2: asynchronous state, out-of-phase synchronous state, almost in-phase chaotic synchronous state and in-phase synchronous state. The left column represents the phase portraits on $(V_1,\ V_2)$ plane. In the right column, the blue solid and red dashed lines represent the action potentials of neuron 1 and neuron 2, respectively.

When $g_c = 0.0027$ nS, the coupled neurons present an asynchronous state with irregular firing patterns and the corresponding phase portraits are chaotic (Fig. 2(a)). An out-of-phase synchronous state emerges when $g_c = 0.018$ nS (Fig. 2(b)). Under these circumstances, the neurons produce bursting patterns and the time series of the membrane potential are the same in shape, but the phase differences between them constantly range from 0 to 2π. With further increase of g_c, an almost in-phase chaotic synchronous state appears (Fig. 2(c) and (d)). In this case, the

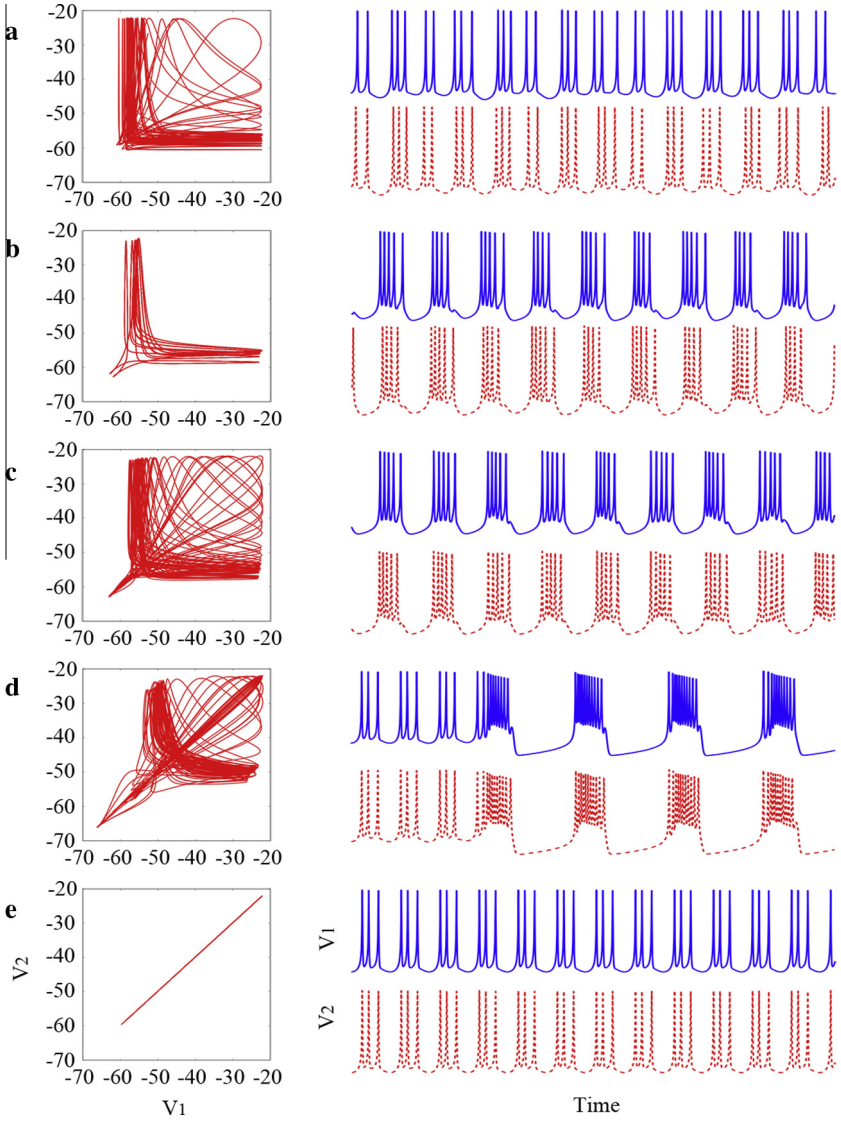

Fig. 2. Phase diagrams of V_1 versus V_2 in mV (left column) and action potential traces for both neurons (right column) for different values of the coupling strength. (a) Asynchronous state ($g_c = 0.0027$ nS), (b) out-of-phase synchronous state ($g_c = 0.018$ nS), (c) almost in-phase chaotic synchronous state ($g_c = 0.0243$ nS), (d) almost in-phase chaotic synchronous state ($g_c = 0.0792$ nS), (e) in-phase synchronous state ($g_c = 0.09$ nS).

phase differences are rather close to 0 or 2π. As g_c increases to 0.09 nS, the neurons present an in-phase synchronous state (Fig. 2(e)). In this case, the impulse patterns appear identical at the same time ($\Delta\varphi = 0$ or 2π), and this implies that the neurons are fully synchronized.

4.2. Role of the slow time constant with constant coupling strength

Fixing the coupling strength $g_c = 0.0036$ nS, we research the effect of the slow time constant τ_s on phase differences ($\Delta\varphi$) and interspike intervals (ISI) as shown in Fig. 3. Fig. 3 consists of the following three parts: the phase differences (top section), interspike interval distribution for the coupled neurons (middle section) and interspike intervals of uncoupled or in-phase synchronous neurons (bottom section) for comparison.

Variations in the firing patterns are closely associated with variations in the phase differences. More specifically, the phase differences are distributed in lines when this is the same in the plots of the interspike intervals and the phase differences are irregularly distributed when the interspike intervals present chaotic dynamics.

Firstly, with increase of τ_s in low values, such as $\tau_s \in [2000, 6500]$, firing patterns present spiking switching to period-2 pattern with an in-phase synchronous state. When the neurons present in-phase synchronization, the distribution of coupled neurons interspike intervals are the same as that of uncoupled neurons. Then, the coupled neurons exhibit irregular distribution of both phase differences and interspike intervals, for example $\tau_s \in [6500, 11, 560]$. In contrast, the uncoupled neurons still exhibit bursting patterns from period-2 to period-4 activity. With further increase of τ_s, such as $\tau_s \in [11, 560, 14, 640]$, an out-of-phase synchronous state appears which alternates with asynchronous behavior, while the uncoupled neuron produces chaotic activity. With further increasing τ_s, for instance $\tau_s \in [14, 640, 19, 000]$, both the distribution of phase differences and interspike intervals become irregular again. In this regime, the individual neuron's firing pattern is chaotic passing through a period-doubling bifurcation area (from period-3 activity turning into period-6 activity).

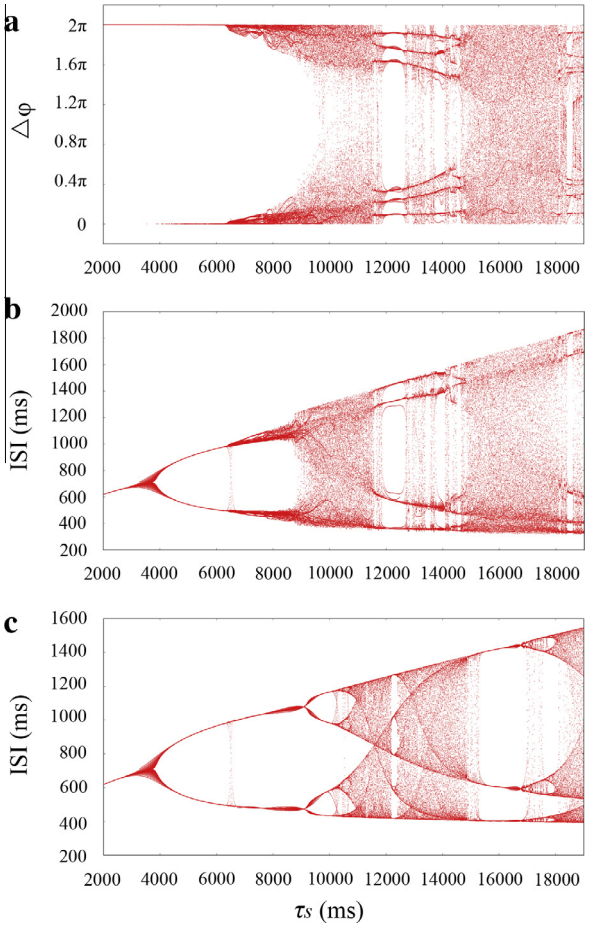

Fig. 3. Bifurcation diagrams of phase differences ($\Delta\varphi$) and interspike intervals (ISI) on the slow time constant scaling. (a) Plots of phase differences at constant coupling strength ($g_c = 0.0036$ nS) with variation of the parameter τ_s; (b) the corresponding variations of the interspike intervals (ISI); (c) the interspike intervals of uncoupled or in-phase synchronous neurons.

4.3. Diagram of synchronous areas and spike-counting on the (g_c, τ_s) plane

For the synchronization research, we use the coupling strength (g_c) and the slow time constant (τ_s) as control

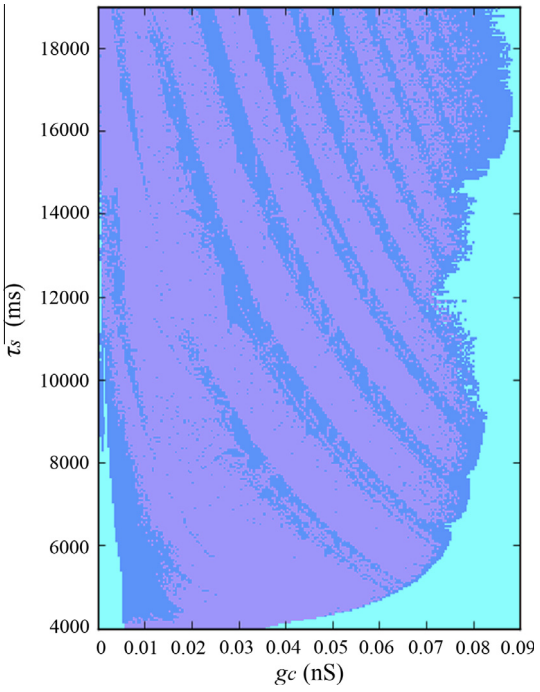

Fig. 4. The map of synchronous states for two coupled neurons on the plane: coupling strength (g_c) and the slow time constant (τ_s). The light green area represents the region of in-phase synchronization. The blue area stands for the region of out-of-phase synchronization. The violet area denotes the region of asynchronization. (For interpretation of the references to color in this figure legend, the reader is referred to the web version of this article.)

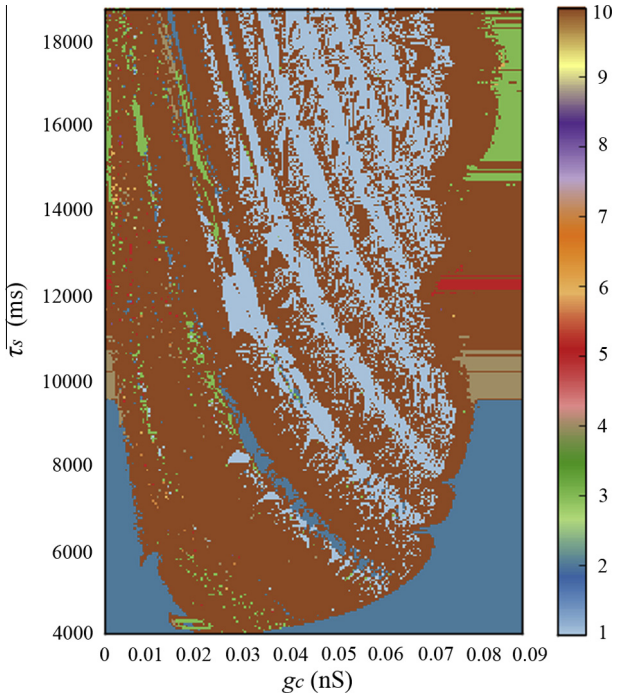

Fig. 5. Spike-counting (SC) diagram of the coupled neurons. The color-coded bar in the right column denotes the number of spikes per burst. The number 1 presents tonic-spiking; regular bursting is expressed by number 2–9, while the number 10 indicates chaotic bursting. (For interpretation of the references to colour in this figure legend, the reader is referred to the web version of this article.)

parameters. The synchronized states can be determined by the phase differences between the adjacent spiking times of the two coupled neurons. By this method we can distinguish different synchronized states combining the coupling strength and the slow time constant as indicated in Fig. 4.

The diagram is divided into different regions according to the three major synchronous states. From the figure, we can find two in-phase synchronization regions characterized by light green color scattered on the $(g_c,\ \tau_s)$ plane. Both at low and high coupling strength, two neurons can accomplish in-phase synchronized state. Furthermore, when the neurons are at the highest coupling strength regime they could promptly go into in-phase synchronization with $\tau_s \in [4000, 19,000]$. All these states can be observed by increasing coupling strength and the slow time constant. It's worth noting that a particular region of asynchronous and out-of phase synchronous behavior emerges. In this region, asynchronous and out-of-phase synchronous states appear alternately and form several similar band-type areas.

Fig. 5 presents the $(g_c,\ \tau_s)$-parameter diagram of spike-counting (SC) of the coupled neurons. The color-coded bar on the right gives the range of spike-numbers. By combining Figs. 4 and 5, we can find that: (1) In-phase synchronization can be achieved not only in regular bursting regions, but also in chaotic bursting regions. (2)

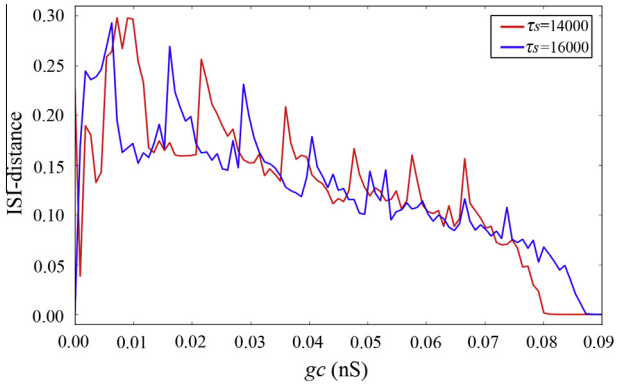

Fig. 6. Dependence of ISI-distance on the coupling strength g_c for two values of the slow time constant τ_s (in ms): 14,000 (red), 16,000 (blue). (For interpretation of the references to color in this figure legend, the reader is referred to the web version of this article.)

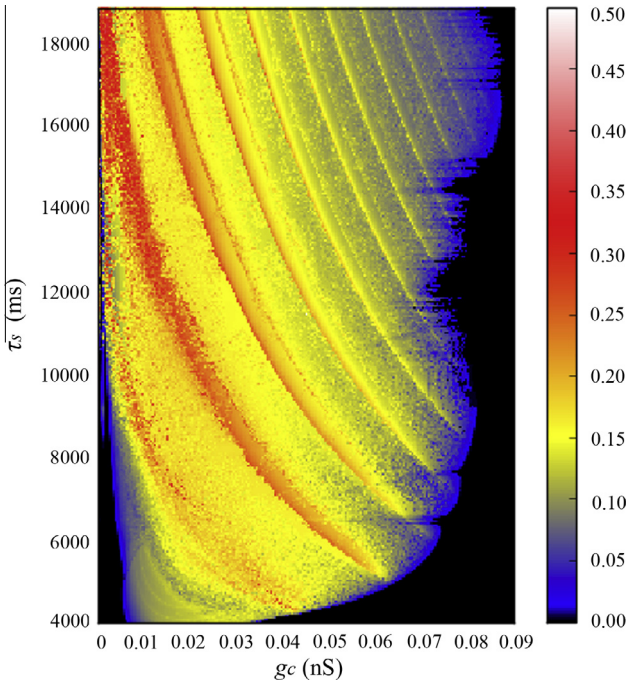

Fig. 7. Plots of ISI-distance in dependence on the coupling strength g_c and the slow time constant τ_s. The scale in the right column indicates that different ISI-distance values are denoted by different color intensities. The in-phase synchronous state is denoted by the black area and the out-of-phase synchronous state is denoted by the blue area. (For interpretation of the references to color in this figure legend, the reader is referred to the web version of this article.)

The coupled neurons are more inclined to enter an out-of-phase synchronization state in tonic-spiking regions. (3) Asynchronization is always accompanied by chaotic bursting.

4.4. Research of synchronization and transitions by the ISI-distance

The above analyses show several synchronous phenomena. But, how can we estimate the degree of synchrony between two coupled neurons? Here, we adopt the ISI-distance, which is a complementary method of extracting the timing of spikes and computing the ratio of transient firing rates. Complete synchronization takes place if $DI = 0$.

In Fig. 6, we give the specific variations on the ISI-distance, which is calculated as defined by Eq. (11), as a continuous function of the coupling strength for two values of the slow time constant. In order to generalize the above acquired results, we scatter the values of DI in a two-dimensional parameter space. As shown in Fig. 7, the dependence of DI on the coupling strength g_c and the slow time constant τ_s is exhibited. The color intensity describes the synchronized degree of the coupled neurons. Specifically, deeper color representing smaller a DI value which indicates a higher degree of synchronization between the coupled neurons. It is obvious that there exist two black regions of DI, where the in-phase synchronization can be realized. The blue regions representing the out-of-phase synchronization are surrounding the black areas, which coincide with Fig. 4. Yellow and red regions alternately appear in the remaining area, which indicate that DI sometimes increases, and sometimes decreases (compare curves for $\tau_s = 14,000$ and for $\tau_s = 16,000$ in Fig. 6). From Fig. 7, we can see that both for smaller and larger g_c, complete synchronization can be obtained. When g_c is large enough, for example $g_c = 0.09$, the coupled neurons immediately go into in-phase synchronization for any finite τ_s.

5. Conclusions

In conclusion, we have used two computational approaches to examine how the different synchronous and asynchronous states propagate and modify neuronal firing patterns. In the present research, we have systematically analyzed the propagations between different synchronous states as functions of the coupling strength and the slow time constant. From these results, we have several conclusions as follows:

(1) The analysis of bifurcation and phase plane obviously show that synchronization transmission goes along with the transition of impulse patterns. Specifically, the impulse patterns of coupled neurons are quite different from that of the single neuron as long as the coupled neurons are not in-phase synchronized.
(2) An appropriately adjusted coupling strength can significantly destroy or promote synchronous states. Indeed, both for smaller and larger coupling strengths, in-phase synchronization can be realized.
(3) Compared with the phase differences method, the approach of ISI-distance can not only distinguish three distinct synchronization states, but also characterize the degree of the same synchronization states.

Both of the methods mentioned above are based on the time intervals between continuous spikes rather than the measurement of the independent elements of two spike trains. These methods are parameter-free, timescale-independent and can naturally characterize the neuronal spike trains. Because of the self-adaptation of these methods, they serve as a time-resolved manner to depict the degree of synchrony between two spike trains. Furthermore, they yield good results even on a limited range of time scales. Thus, we only need to choose a length of stable firing patterns to compute the synchronous indexes, which saves a great deal of time. We believe that these methods are profound and instructive for further research on synchronization states of different types of coupled neurons or multiple coupled neurons.

Acknowledgment

This work was supported by the National Natural Science Foundation of China under Grant No. 11172103.

References

[1] Levy R, Hutchison WD, Lozano AM. High-frequency synchronization of neuronal activity in the subthalamic nucleus of parkinsonian patients with limb tremor. J Neurosci 2000;20(20):7766–75.
[2] Mormann F, Kreuz T, Andrzejak RG. Epileptic seizures are preceded by a decrease in synchronization. Epilepsy Res 2003;53(3):173–85.
[3] Arenas A, Diaz-Guilera A, Kurths J. Synchronization in complex networks. Phys Rep 2008;469(3):93–153.
[4] Volman V, Perc M, Bazhenov M. Gap junctions and epileptic seizures – two sides of the same coin? PLoS One 2011;6(5):e20572.
[5] Wang Q, Chen G, Perc M. Synchronous bursts on scale-free neuronal networks with attractive and repulsive coupling. PLoS One 2011;6(1):e15851.
[6] Zhang X, Wang R, Zhang Z. Dynamic phase synchronization characteristics of variable high-order coupled neuronal oscillator population. Neurocomputing 2010;73(13):2665–70.
[7] Wang H, Wang Q, Lu Q. Bursting oscillations, bifurcation and synchronization in neuronal systems. Chaos Solitons Fract 2011;44(8):667–75.
[8] Wang Q, Lu Q, Chen GR. Bifurcation and synchronization of synaptically coupled FHN models with time delay. Chaos Solitons Fract 2009;39(2):918–25.
[9] Postnova S, Voigt K, Braun HA. Neural synchronization at tonic-to-bursting transitions. J Biol Phys 2007;33(2):129–43.
[10] Pikovsky A, Rosenblum M, Kurths J. Synchronization: a universal concept in nonlinear sciences. Cambridge: Cambridge University Press; 2001.
[11] Ermentrout B. Type 1 membranes, phase resetting curves, and synchrony. Neural Comput 1996;8(5):979–1001.
[12] Chow CC, Kopell N. Dynamics of spiking neurons with electrical coupling. Neural Comput 2000;12(7):1643–78.
[13] Hansel D, Mato G, Meunier C. Synchrony in excitatory neural networks. Neural Comput 1995;7(2):307–37.
[14] Hestrin S. The strength of electrical synapses. Science 2011;334(6054):315–6.
[15] Bennett MVL. Electrical synapses, a personal perspective (or history). Brain Res Rev 2000;32(1):16–28.
[16] Greengard P. The neurobiology of slow synaptic transmission. Science 2001;294(5544):1024–30.
[17] Galarreta M, Hestrin S. A network of fast-spiking cells in the neocortex connected by electrical synapses. Nature 1999;402(6757):72–5.
[18] Liu C, Wang J, Wang L. Multiple synchronization transitions in scale-free neuronal networks with electrical and chemical hybrid synapses. Chaos Solitons Fract 2014;59:1–12.
[19] Wang J, Guo X, Yu H. Stochastic resonance in small-world neuronal networks with hybrid electrical–chemical synapses. Chaos Solitons Fract 2014;60:40–8.
[20] Sun J, Deng B, Liu C. Vibrational resonance in neuron populations with hybrid synapses. Appl Math Model 2013;37(9):6311–24.
[21] Mosekilde E, Lading B, Yanchuk S. Bifurcation structure of a model of bursting pancreatic cells. BioSystems 2001;63(1):3–13.
[22] Lading B, Mosekilde E, Yanchuk S. Chaotic synchronization between coupled pancreatic-cells. Prog Theor Phys Suppl 2000;139:164–77.
[23] Sherman A, Rinzel J. Model for synchronization of pancreatic beta-cells by gap junction coupling. Biophys J 1991;59(3):547–59.
[24] Wang QY, Lu QS, Chen GR. Ordered bursting synchronization and complex wave propagation in a ring neuronal network. Phys A Stat Mech Appl 2007;374(2):869–78.
[25] Sherman A, Rinzel J, Keizer J. Emergence of organized bursting in clusters of pancreatic beta-cells by channel sharing. Biophys J 1988;54(3):411–25.
[26] Kreuz T, Haas JS, Morelli A. Measuring spike train synchrony. J Neurosci Methods 2007;165(1):151–61.
[27] Kreuz T, Chicharro D, Andrzejak RG. Measuring multiple spike train synchrony. J Neurosci Methods 2009;183(2):287–99.
[28] Kreuz T, Chicharro D, Greschner M. Time-resolved and time-scale adaptive measures of spike train synchrony. J Neurosci Methods 2011;195(1):92–106.